Asian Journal Science and Engineering

Vol. 2, No. 2, December 2023
https://attractivejournal.com/index.php/ajse

Cathodic Corrosion Protection on Low Carbon Steel Type H-beam (SM490YB) Using Zinc (Zn) Anode with Soil Corrosive Media Mixed with NaCl

Lazuardi[1], Muhammad Akhlis Rizza[2*], Sugeng Hadi Susilo[3], Maryono[4]
[1,2] Politekhnik Negeri Malang, Indonesia

atingthok99@gmail.com*

ARTICLE INFO
Article history:
Received
October 01, 2023
Revised
December 20, 2023
Accepted
December 31, 2023

Abstract

H-beam steel is often used as a basic material for building construction on the coast. Cases that often occur are H-beam steel that is installed quickly corrodes. This incident is caused by the coastal area belongs to an environment with a high level of corrosiveness.From the results of the pH tester test, the value of the degree of acidity is in rangeof pH=5 to pH=7.Coastal soils contain a lot of chloride Cl. In an acidic environment accompanied by a chloride Cl element, it triggers the breakdown of the passive layer on the surface which causes an anodic region to form so that the steel is in a state of releasingFe^{2+} electrons. The problem that occurs can be overcome using a sacrificial anode cathodic protection system, with a zinc metal protection mechanism (Zn) 99, 99% which is used as a sacrificial anode has a lower potential value than the potential value of H-beam steel as a cathode protected by zinc metal (Zn) $E^{\circ} = -0{,}76\ volt$. This value of zinc metal (Zn) is more negative than the Fe steel which potential value is $E^{\circ} = -0{,}44\ volt$. The value of the potential difference is $E^{\circ}\ sel = +0{,}32$that it can be ascertained that the released Zn electrons can flow and adhere to the protected H-beam steel.

Keywords: Surface Corrosion, Cathodic Protection, H-beam Steel, Zinc Anode(Zn)

Published by CV. Creative Tugu Pena
ISSN 2963-6752
Website https://attractivejournal.com/index.php/ajse

INTRODUCTION

H-beam steel (SM490YB) with a carbon content of 0.2% has malleability and good machinability, and has weldability. It belongs to the low carbon steel group.

Table 1. H-beam steel composition

H-beam steel composition (SM490YB) %				
C	***Si***	***Mn***	***P***	***S***
0,2	0,55	1,65	0,035	0,035

Source: Mill Sertifikat JIS G3106 SM490YB

From (Table 1) is the result of the H-beam (SM490YB) steel composition test, it can be seen that in addition to 0.2% *C* (*carbon*) in the H-beam composition, there are other elements: *Si* (*Silikon*) 0,5%, *Mn* (*Mangan*) 1,65%, *P* (*fosfor*) 0,035%, dan *S* (*Sulfur*) 0,035%.

H-beam Steel Surface is prone to corrosion

The H-beam steel surface that is prone to corrosion is usually located in the peeling paint / protective layer. (Figure1) is an example of corrosion that occurs in the H-beam steel section.

Figure 1. Corrosion on H-beam Steel Surface.

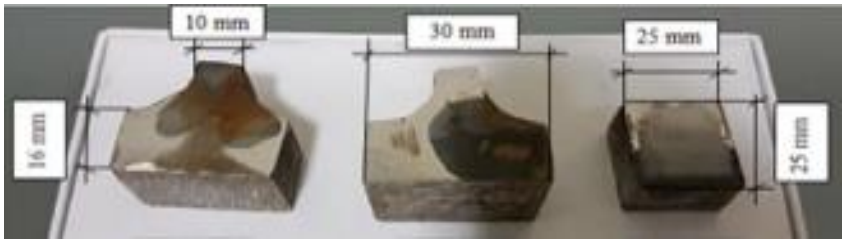

Source: [1]

From the research conducted by this budget, the H-beam steel section which is prone to corrosion is located at the corner of the flange.

Use of H-beam in Industry

H-beam steel (SM490YB) in industry is often used as the main raw material for a building construction, example: used on offshore drilling platforms, harbor bridge construction, and various industrial buildings. The main raw material for construction uses H-beam steel (SM490 YB).

Figure 2. Pasuruan City Fish Auction Center.

Source: documentation in research

(Figure 2**)** is the location of the center of the fish auction industry in the city of Pasuruan. The building construction material is made of H-beam steel. Santina.(2018), buildings designed using WF construction are stronger and resistant to vibration. The critical buckling load of the H-beam profile is 18,295 kN

Figure 3. Eigenvalue buckling pada profil H

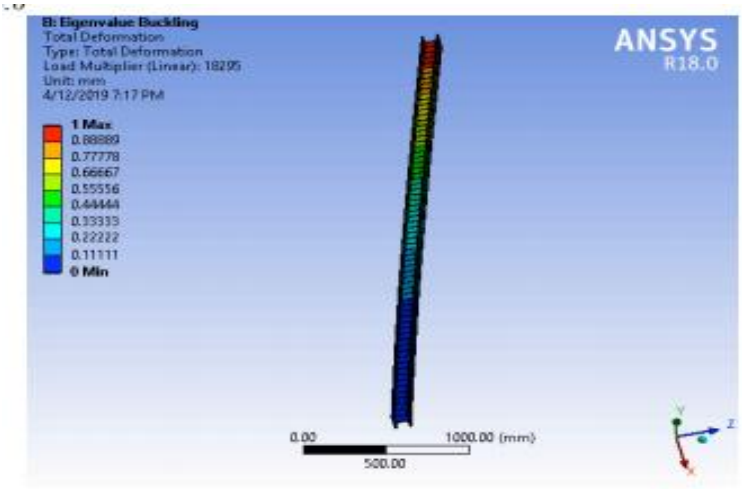

Source: [2]

Corrosion Conditions of Coastal Environment

The environmental conditions of coastal soils contain a lot of *chloride (Cl)* elements*.* acidic environmental conditions accompanied by the element *chloride (Cl),* a steel construction will potentially quickly experience surface corrosion.

Table 2. Elements in Soil

Kandungan Unsur-unsur di Dalam Tanah	
Harga Makro	**Harga mikro**
C, H, O, N, P, K, Ca, Mg dan S	B, Cl, Cu, Fe, Mn, Mo, Na, dan Zn

Source: [3]

Suhariyono.(2005), Soil contains various elements. There are various soil elements that affect the reaction process of corrosion in the environment, namely: *O* (*Oksigen), H* (*Hidrogen),* dan *Cl* (*Clorida) Effect of Elemental Chloride(Cl) on Steel Corrosion.*

Figure 4. Corrosion rate of carbon steel is influenced by NaCl concentration

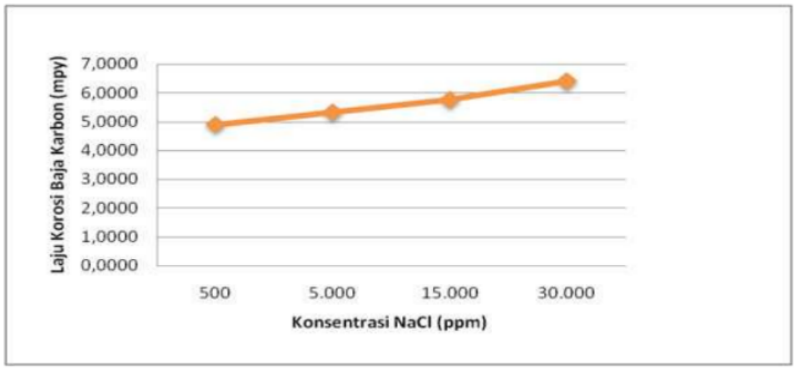

Source: Rahmat [4]

(Figure 4) From the corrosion rate curve, it can be concluded that the concentration of *NaCl* solution affects the corrosion rate of steel, the higher the *NaCl* concentration, the higher the corrosion rate.

Compound Effect of Acid $(H^{+}Cl)$ ***on Corrosion of Steel***

Rukminasari[5], The coastal environment in Indonesia has a degree of acidity in the range of pH = 5 to pH = 8. In cathodic protection environmental pH also affects the rate of corrosion of steel, because in high acidic environmental conditions, $(H^{+}Cl)$ compounds cause more and more Fe atoms to be released to move to the cathodic surface area with a charge of OH^{-} as much as 2 electrons so that the corrosion rate is higher. This can be evidenced by the current investigation of the influence of pH on steel protection Purtra.(2018), environmental pH conditions affect the potential of steel in a corrosive environment. The pH VS Potential (mV) diagram can be seen in (figure 5)

Figure 5. Comparison of the pH value and potential of metal

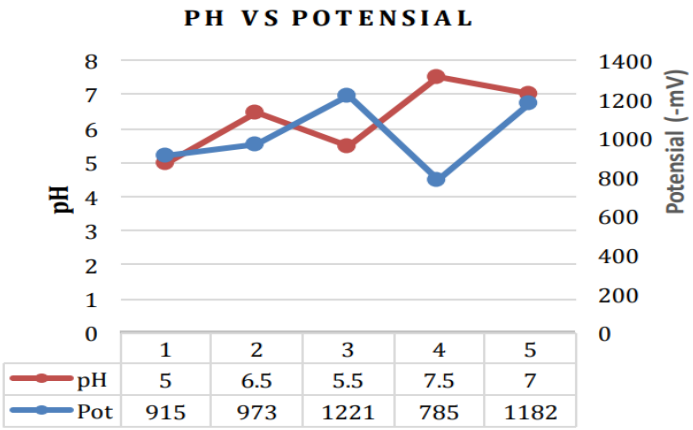

Source: [6]

From the pH vs Potential diagram, it can be explained that the lowest acidity value of pH = 5.5 (acidic solution) has a potential of 1200-mV, while the highest potential value of pH = 7.5 (wet solution) is only 785-mV . So that it can be concluded that under acidic conditions the metal ions are more soluble.

Corrosion Reaction of Steel in Soil.

Loss of electrons in steel or corrosion reactions that occur when Fe^{2+}atoms lose electrons and form hollows on the steel surface (anodic region), Trethewey [7]

$$\longrightarrow \quad Fe \qquad Fe^{Z+} + ze^{-}$$

Notification:

Fe = Atom symbol

z = Number of elektron of an element

The released Fe^{2+} steel electrons will move to the part with a high oxygen concentration (cathode region), the electrons released from the Fe atom reduce O_2. The formation of corrosion on the steel surface, Fe_2O_3 n H_2O, formed in an oxidation-reduction reaction that is different from an electron-loss reaction. The Fe^{2+} atom in the anode region is dispersed by water so that a reaction occurs with O_2 to form Fe^{3+}in rust.

Reaction formation of rust on the steel surface , Trethewey.(1991), As follows:

$$2Fe^{2+} + \frac{1}{2}O_2 + (2+n)H_2O$$

Becomes

$$Fe_2O_3.nH_2O + 4H^+$$

Steel with Zinc Coating Protection

Figure 6. Corrosion Rate of Steel with Al and Zn coating in NaCl

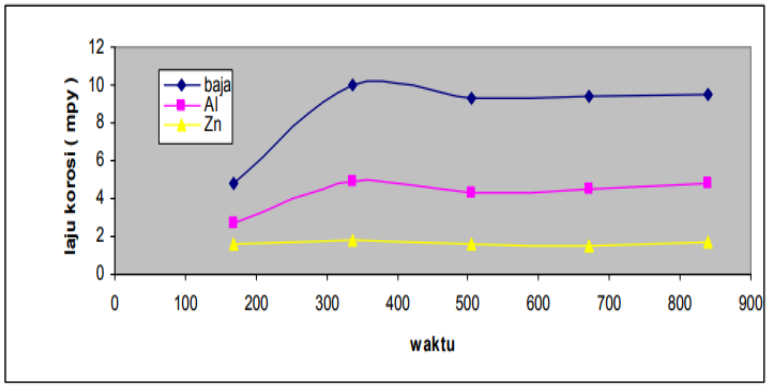

Source: Utami,(2009)

Figure 7. Cathodic Protection Design

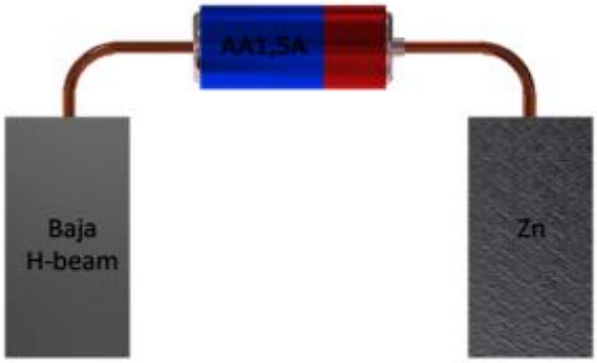

(figure 6) is a Zn (Zinc) coating protection on the steel surface. From the corrosion rate curve, it is explained that in a time span of 168 hours the corrosion rate of steel is 2.7 *mpy* the corrosion rate is low because the steel surface is still coated with Zn. After a running time span of 336 hours the corrosion rate of steel has increased by 4.8 *mpy*, this increase in corrosion rate occurs because the zinc layer has been corroded, in a span of 504 hours the surface is in a condition that is no longer protected. It can be concluded that protection with a coating system only delays when a constant corrosion rate occurs, Therefore, it is necessary to add cathodic protection to the steel surface so that the steel surface is always in a protected state. as in the example in (Figure 7)

Anode *Zinc (Zn)* 99.99%.

Zinc metal Zn 99.99% as a sacrificial anode has a lower potential value than the potential value of the protected H-beam steel.

Figure 8. Anode *Zinc (Zn)* 99,99%

Source: documentation in research

Table 3. List of Potential To Metal

Metal Type	*E° volt*
Zn	-0,76
Cr	-0,71
Fe	-0,44

Source: Fontana.(1986)

From (table 3), it can be found that the potential value of zinc metal Zn, E° = - 0.76 volts, this value is more negative than that of steel Fe whose potential value is E° = - 0.44 volts. It can be seen the difference in cell potential between Fe and Zn as in the following calculation:

$$E^{\circ}\, sel = E^{\circ}\, Fe - E^{\circ}\, Zn$$

$$E^{\circ}\, sel = -0{,}44\ volt - (-0{,}76\ volt)$$

$$E^{\circ}\, sel = -0{,}44\ volt + 0{,}76\ volt$$

$$E^{\circ}\, sel = +0{,}32$$

The value of the potential difference between Zn and Fe is E° cell = + 0.32. It can be ascertained that the released Zn electrons flow towards the H-beam steel (Fe metal).

METHODS

This type of research is viewed from the design of this study using an experimental method with an Intact-Group Comparison design [8][9]. The research design consists of two groups[10]. The first group was used as control (H-beam steel without cathodic protection treatment), while the second group was used for experiment (H-beam steel was cathodic protected using 99.99% Zn anode).

Research Design Draft

Experimental research method as a research method used to find the effect of certain treatments[11] under controlled conditions[12][13]. the research design can be seen in (Figure 9).

Figure 9. Research Design Diagram

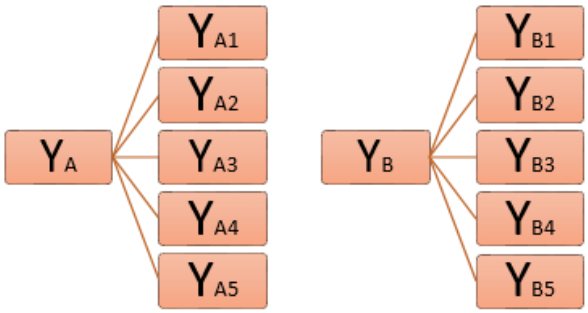

Notification :

$YA_{1\ sd\ 5}$ = H-beam steel without cathodic protection treatment.

$YB_{1\ sd\ 5}$ = H-beam steel was cathodic protected using 99.99% Zn anode.

Two experiments were carried out on the corrosion rate value of H-beam steel (SM490YB) without cathodic protection with specimen code ($YA_{1\ sd\ 5}$) and experiments on the corrosion rate value of H-beam steel (SM490YB) with cathodic protection with specimen code ($YB_{1\ sd\ 5}$).

Design of Cathodic Protection in Research

Zinc (Zn) anode is mounted on the positive pole and the H-beam steel as a protected cathode is mounted on the negative pole. This is done so that the released Zn electrons are directed towards the surface of the protected H-beam steel. protection design circuit can be seen in (Figure 10)

Figure 10. Closed circuit electric current.

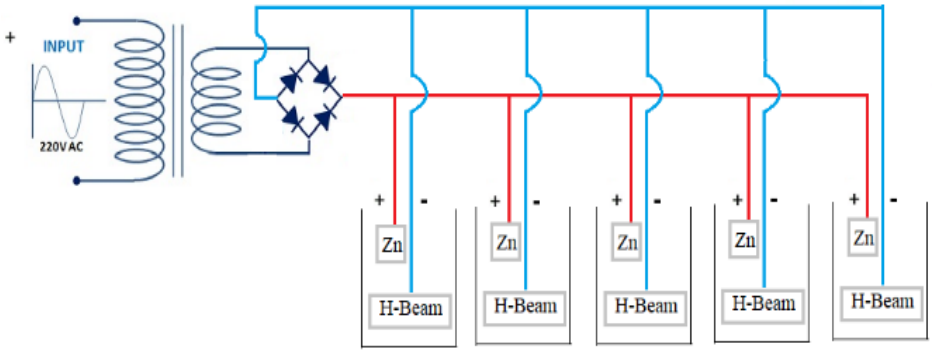

Source: documentation in research

RESULT AND DISCUSSION

Corrosion rate calculation data were carried out on specimens Y_{A1} to Y_{A5} (without protection) and specimens Y_{B1} to Y_{B5} (protected) with time variations of

144 hours, 288 hours, 432 hours, 576 hours, 720 hours, for 30 days. The form of protection can be seen in (Figure 11)

Figure 11. Forms of Cathodic Protection.

Source: documentation in research

Acidity Test of the Coastal Environment

In the coastal soil environment, acid and alkaline reactions will occur, this is influenced by the concentration of H^+ and OH^- ions contained in the soil.

Figure 12. Acidity Test of the Coastal Environment.

Source: documentation in research

The natural acidity values in the coastal environment when measured using a pH meter at three different points can be seen in (Table 4).

Table 4. pH Value of the Coastal Natural Environment

Location	Acidity Level (pH)
Beach	5 – 6
Mangrove forest	6 – 6,5
Beachside Industry	6 – 7

Source: Field observation results

The pH value of the soil acidity after being put into the experimental glass for a time variation of 144 hours, 288 hours, 432 hours, 576 hours, 720 hours. It can be seen in (Table 5).

Table 5. pH values during the experiment.

Time (hours)	pH
144	6
288	6,5
432	6
576	6
720	6

Source: Field observation results

From table 5, it can be shown that the acidity value curve of soil pH during the experiment with time variations of 144 hours, 288 hours, 432 hours, 576 hours, 720 hours, for 30 days. Can be seen in (Figure 13)

Figure 13. Graph of pH during the experiment.

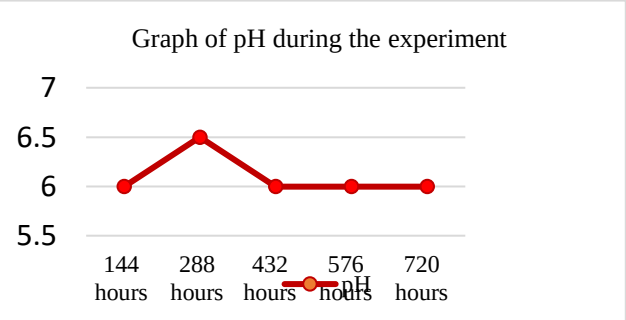

Losing weight on a steel H-beam Without Protection.

The value of weight loss that occurs in H-beam steel (SM490YB) in bare conditions without protection in the corrosive environment of coastal estuary sand reinforced with a mixture of NaCl. Can be seen in (Table 6)

Table 6. Weight Loss of H-beam Steel (SM490 YB) Without Protection.

Code		Time (*Hours*)	Losing Weight (g)	Rate Corrosion (mpy)
Y_{A1}	$Y_{A1.1}$	144	0,050	6,915
	$Y_{A1.2}$		0,050	6,915
	$Y_{A1.3}$		0,050	6,915
Y_{A2}	$Y_{A2.1}$	288	0,090	6,223
	$Y_{A2.2}$		0,110	7,606
	$Y_{A2.3}$		0,090	6,223
Y_{A3}	$Y_{A3.1}$	432	0,160	7,376
	$Y_{A3.2}$		0,160	7.376
	$Y_{A3.3}$		0,160	7,376
Y_{A4}	$Y_{A4.1}$	576	0,230	7,952

	$Y_{A4.2}$		0,230	7,952
	$Y_{A4.3}$		0,230	7,952
Y_{A5}	$Y_{A5.1}$	720	0,310	8,574
	$Y_{A5.2}$		0,310	8,574
	$Y_{A5.3}$		0,310	8,574

Source: Findings in Research

From (Table 6), a diagram of the mass loss value of H-beam (SM490YB) steel without protection can be presented.

Figure 14. Diagram of the specimen weight loss without protection

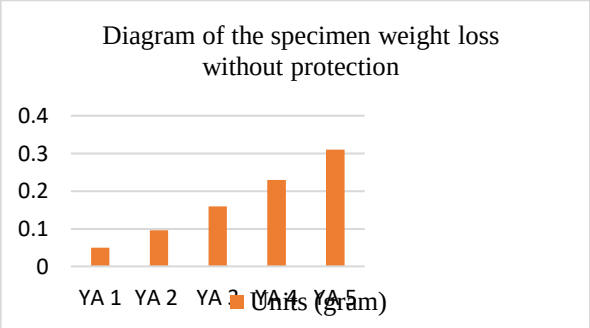

Source: Findings in Research

Corrosion rate of steel H-beam without protection.

corrosion rate using units of Mils per year (*mpy*) at the corrosion rate unit desire value of $3{,}45 \times 10^6$. At various time variations 144 hours, 288 hours, 432 hours, 576 hours, 720 hours, for 30 days. Data on the corrosion rate of unprotected H-beam steel can be seen in (Table 7).

Table 7. Corrosion rate of steel H-beam without protection.

Code	Time (*Hours*)	Losing Weight (*gram*)	Rate Corrosion (mpy)
Y_{A1}	144	0,050	6,915
Y_{A2}	288	0,096	6,684
Y_{A3}	342	0,160	7,376
Y_{A4}	576	0,230	7,952
Y_{A5}	720	0,310	8,574

Source: Findings in Research

From (table 7) describes the corrosion rate curve of H-beam steel (SM490YB) without protection for 30 days.

Gambar 15. Grafik Laju Korosi Spesimen Tanpa Proteksi.

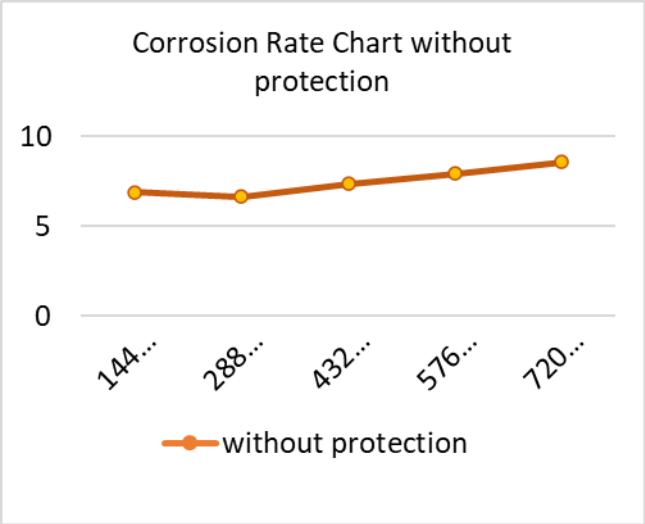

Source: Findings in Research

Loss of weight in H-beam Steel Protected by Zinc (Zn) Anodes.

The value of weight loss that occurs in H-beam steel (SM490YB) in bare conditions with protection in the corrosive environment of coastal estuary sand reinforced with a mixture of *NaCl*. Can be seen in (Table 8)

Table 8. Heavy Loss Data of H-beam (SM490YB) Protected Steel.

Code		Time (*Hours*)	Losing Weight (g)	Rate Corrosion (mpy)
Y_{B1}	$Y_{B1.1}$	144	0,040	0,036
	$Y_{B1.2}$		0,040	
	$Y_{B1.3}$		0,030	
Y_{B2}	$Y_{B2.1}$	288	0,070	0,063
	$Y_{B2.2}$		0,060	
	$Y_{B2.3}$		0,060	
Y_{B3}	$Y_{B3.1}$	432	0,090	0,093
	$Y_{B3.2}$		0,100	
	$Y_{B3.3}$		0,090	
Y_{B4}	$Y_{B4.1}$	576	0,120	0,120
	$Y_{B4.2}$		0,130	
	$Y_{B4.3}$		0,110	
Y_{B5}	$Y_{B5.1}$	720	0,160	0,153
	$Y_{B5.2}$		0,140	
	$Y_{B5.3}$		0,160	

Source: Findings in Research

From (Table 8) it can be presented through a diagram that will describe the mass loss value of H-beam steel (SM490YB) protected by zinc anode (Zn).

Figure 16. Weight loss diagram of *Zn* diagram anode protected h-beam steel.

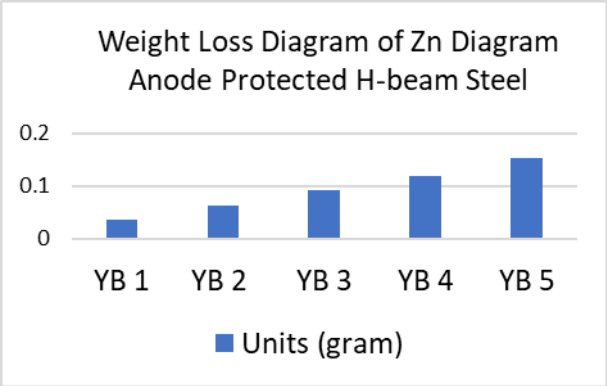

Source: Findings in Research

Corrosion Rate of H-beam Steel Specimens Protected by Zinc Anode (Zn).

corrosion rate using units of Mils per year (*mpy*) at the corrosion rate unit desire value of $3{,}45 \times 10^{6}$. At various time variations 144 hours, 288 hours, 432 hours, 576 hours, 720 hours, for 30 days. Data on the corrosion rate of H-beam protected steel can be seen in (Table 9).

Tabel 9. Laju Korosi Baja H-beam Diproteksi.

Code	Time (*Hours*)	Losing Weight (*gram*)	Rate Corrosion (mpy)
Y_{B1}	144	0,036	5,071
Y_{B2}	288	0,063	4,379
Y_{B3}	342	0,093	4,320
Y_{B4}	576	0,120	4,149
Y_{B5}	720	0,153	4,241

Source: Findings in Research

From table 9 it can be presented through a graph that will describe the corrosion rate curve of H-beam steel (SM490YB) protected by zinc anode (Zn) for 30 days. The corrosion rate curve of the protected steel specimen can be seen in (Figure 17).

Figure 17. Corrosion rate of Protected H-Beam steel.

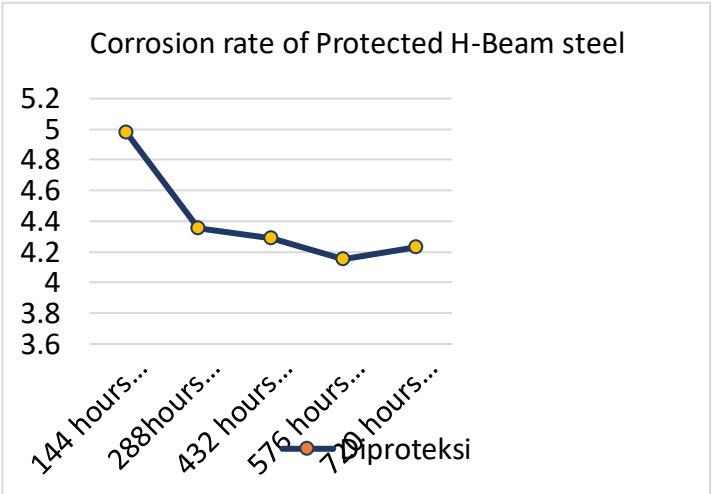

Corrosive Environmental Analysis

The pH value of the acidity obtained in the coastal environmental conditions of Pasuruan City is between pH 5 to pH 7

The difference in pH acidity values in the three coastal environments occurs due to various stability factors of content fluctuations of O_2withCO_2in the natural coastal environment [5][14][15][16]

Classification of H-beam Corrosivity Conditions in the Coastal Environment

H-beam steel corrosive conditions can be classified using a pourbaix diagram. described in (Figure 18)

Figure 18. E/pH diagram for iron in water

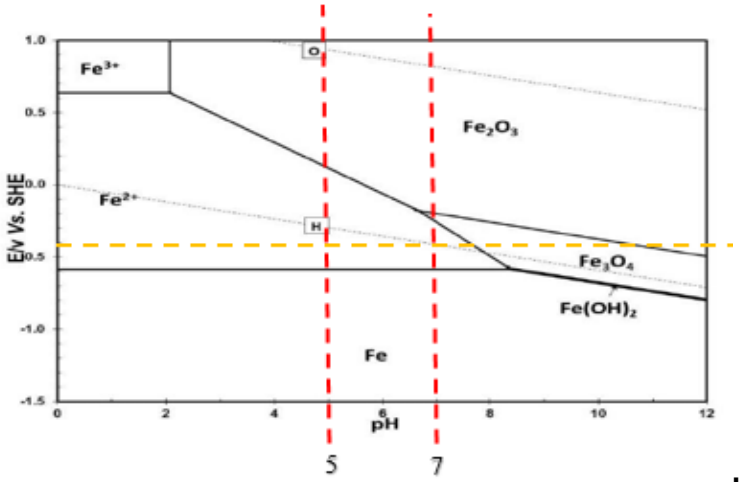

Source: [7]

H-beam steel when seen in the table for the voltaic series E, the potential value of iron is at number $Fe = -0{,}44\ volt$. In the coastal environment with an acidity level between pH 5 to pH 7, H-beam steel will likely experience three conditions, which are the condition of *Fe* the H-beam steel will be in an immune condition, theFe^{2+} condition of the H-beam steel will be in a corrosive condition Fe will release 2 electrons, the condition Fe_2O_3andFe_3O_4, and the H-beam steel will be in a stable state.

Conditions of Zinc Zn Anode in the Coastal Environment.

We can find out the condition of zinc Zn metal as an anode in the environment in the pourbaix diagram described in (Figure 19).

Figure 19. E/pH diagram for Zn in water.

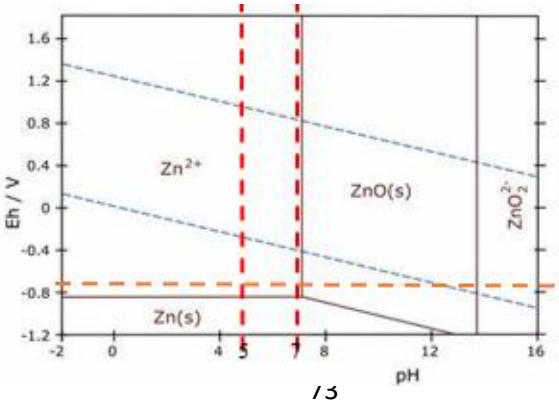

Source: Trethewey, (1991)

Zinc metal Zn 99.99% if seen in the table for the series E volta, the potential value is at number of$Zn = -0{,}75\ volt$. There will be Zn^{2+} state of zinc metal Zn which is in a state of releasing 2 electrons. The electrons released from the Zn anode will be used as a substitute for the loss of corroded Fe electrons in the protected environment.

Analysis of the corrosion rate of H-Beam SM490YB Steel for 144 hours.

Figure 20. Specimen corrosion results for 144 hours.

Source: Research Documentation.

Within 144 hours, the pH of the corrosive medium = 6, and what happened to the specimen without protection$Y_{A\,1}$ lost 0.050 $gram$ with a corrosion rate of 6.915mpy. Meanwhile, the protected specimen with a voltage of E = 1.32 V and a protection current of – 1333 mA lost 0.036 $gram$ with a corrosion rate of 5.071 y . The protected H-beam steel decreased its corrosion rate by 26.6% compared to the unprotected H-beam steel. In the first week, the percentage of the effectiveness of the Zn anode to inhibit the corrosion rate was still low.

This was caused by the zinc (Zn) particles which were still trying to penetrate the sand pores, and some of the zinc (Zn) particles stick to the sand particles which contain a lot of Fe iron. Some researchers stated that in micro units of soil there are elements B[17], Cl[18], Cu[19], Fe[20], Mn[21], Mo[22], Na[23], and Zn [24]. In general, there are various elements that affect the reaction process of corrosion in an environment, including: O (Oxygen), H (Hydrogen), and Cl (Cloride).

Analysis of the corrosion rate of H-Beam SM490YB Steel for 288 hours.
Figure 21. Specimen corrosion results for 288 hours.

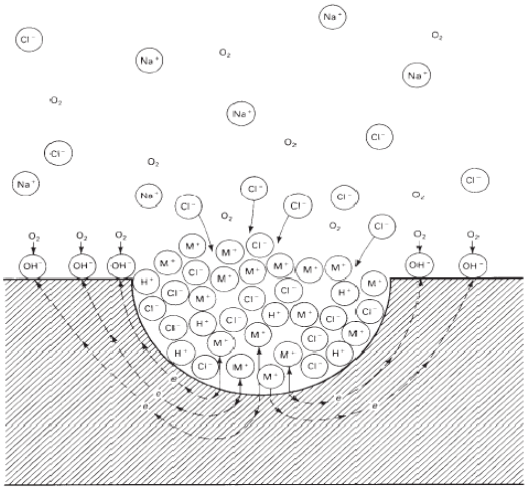

Source: Research Documentation.

Within 288 hours, pH = 6.5 which occurred in the unprotected specimen $Y_{A\,2}$lost 0.096$gram$ with a corrosion rate of 6.684mpy while the protected specimen with a voltage of E = 1.37 V and a protection current of - 1626 mA lost 0.063 $gram$with a corrosion rate of 4.379mpy. The corrosion rate of the protected H-beam steel ($Y_{B\,2}$)decreased its corrosion rate by 34.4% from the unprotected H-beam steel, zinc (Zn) particles began to cover the steel surface but were not covered evenly, and in H-beam steel specimens without protection($Y_{A\,2}$), the corrosion rate decreased. This happened because the pH value increased along with the evaporation of water in the experimental glass.

Figure 22. Release due to compound

Source: Fontana, (1984).

It can be illustrated in (figure 18) that environmental pH affects the corrosion rate of steel. This is because the lower the pH, the more acidic the solution is. If H^+ compounds with more chloride Cl^-elements in the environment, the more atoms that are released will move to the cathodic surface area with $OH^-$of 2 electrons so that the corrosion rate is higher.

Analysis of the corrosion rate of H-Beam SM490YB Steel for 432 hours.

Figure 23. Specimen corrosion results for 432 hours.

Source: Research Documentation.

Within 432 hours, at pH = 6, the unprotected specimen$Y_{A\,3}$ lost 0.160 $gram$with a corrosion rate of 7.376mpy while the protected specimen $Y_{B\,3}$with a voltage of E = 1.32 V and a protection current of – 1685 mA lost 0.093 $gram$with a corrosion rate of 4.320mpy. The corrosion rate of protected H-beam steel$(Y_{B\,3})$ decreased by 41.4% compared to the unprotected H-beam steel, zinc (Zn) particles began to appear evenly covering the steel surface, and the H-beam steel specimens without protection$(Y_{A\,3})$ experienced an increase in the corrosion rate which caused small holes appeared on the surface of the specimen. According to Rahmat [4] The higher the concentration of chloride ions (Cl), the higher the possibility of damage to the protective layer on the metal surface. Chloride ions tend to cause the breakdown of the passive layer, with the mechanism, chloride ions (Cl) penetrate through the passive film layer so that holes are formed and the creation of anodic regions in the form of small holes.

Analysis of the corrosion rate of SM490YB H-Beam Steel for 576 hours.

Figure 24. Specimen corrosion results for 576 hours.

Source: Research Documentation.

Within 576 hours, at pH = 6, the weight loss of the specimen without protection $Y_{A\,4}$was 0.230 $gram$with a corrosion rate of 7.952mpy while the protected specimen$Y_{B\,4}$ with a voltage of E = 1.32 V and a protection current of - 1693 mA lost 0.120 $gram$with a corrosion rate of 4.149mpy. The corrosion rate of the protected H-beam steel $(Y_{B\,4})$decreased its corrosion rate by 47.8% from the unprotected H-beam steel. The shielding current started to stabilize as seen from the difference in

current changes between the 3rd and 4th week wass not so big. In the H-beam steel specimens without protection($Y_{A\,4}$), the corrosion rate increased, pitting corrosion holes were visible on the specimen surface.

SM490YB H-Beam Steel Corrosion Rate Analysis For 720 hours

Figure 25. Corrosion results for 720 hours.

Source: Research Documentation.

Within 720 hours, at pH = 6, the weight loss of the specimen without protection$Y_{A\,5}$ was 0.310 $gram$with a corrosion rate of 8.574 mpywhile the protected specimen $Y_{B\,5}$with a voltage of E = 1.32 V and a protection current of - 1658 mA lost 0.150$gram$ with a corrosion rate of 4.241mpy. The corrosion rate of the protected H-beam steel ($Y_{B\,5}$)experienced 50.5% decrease in its corrosion rate from the unprotected H-beam steel. In H-beam steel specimens without protection($Y_{A\,5}$), the corrosion rate increased.It could be seen that the pitting corrosion holes on the surface of the specimens were getting bigger and bigger**.**

Figure 26. Anodic Region on Specimen Surface.

Source: Research Documentation

On the surface of the unprotected specimen, an increasing anodic area is formed. The anodic area is the holes on the surface where the metal will release Fe^{2+} particles with the corrosion reaction $Fe^{+}Cl^{-} + H_2O = FeOH + H^{+}Cl^{-}$ [25][26][27]. The events that occur in the anodic region on the surface of the specimen can be explained by illustrating the mechanism of the formation of the corrosion reaction. It is explained in (Figure 27) as follows.

Figure 27. Illustration of Corrosion Reaction Area on Specimen Surface.

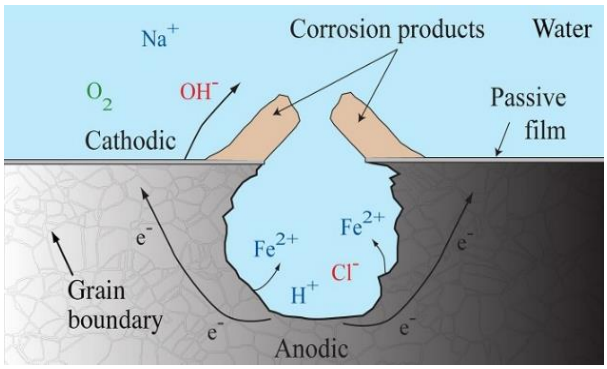

Source: Fontana, (1984).

From Figure 5.15, it can be explained that the mechanism of the formation of a corrosion reaction on the surface of a steel specimen against the elemental chloride Cl in water is as follows:$Fe^{+}Cl^{-} + H_2O$ reaction which will occur $FeOH + H^{+}Cl^{-}$. The nature of the acid solutionH^{+} in compound with the element chlorideCl^{-} tries to penetrate the steel surface, sothe atoms Femove to the cathodic surface area with a chargeOH^{-} of 2 electrons.

CONCLUSION

The research resulted in identification of the corrosion rate that occurred in H-beam Steel SM 490 YB on corrosive media on coastal soil mixed with NaCl solution. The method used in this study is experimental with an intec-group comparison design. Where in this research design, there are two groups. The first group was used as control (H-beam steel without cathodic protection treatment), while the second group was used for experiment (H-beam steel was cathodic protected using 99.99% Zn metal anode). As the result, it can be seen the effects that occur and the results of the given experiment. The conclusions obtained from the research are as follows: **(1)** The value of the corrosion rate of H-beam steel protected using zinc zinc anode for 30 days/720 hours reached 4.241 mpy. The value of the corrosion rate is low due to the cathodic protection system, changing the entire surface of the H-beam steel into a cathodic area by installing the H-beam steel on the negative pole and the entire anodic area being transferred to the zinc metal Zn mounted on the positive pole, the protection current will continue occurs when there is still a zinc Zn anode used as an electron donor. **(2)** The corrosion rate of H-beam steel without protection for 30 days/720 hours reaches 8,574 mpy, the corrosion rate value is higher than that of protected H-beam steel. This happens because at an environmental pH of 6 to 6.5 on the steel surface, two the anodic and cathodic regions. In the anodic region, acid compounds ($H^{+}Cl^{-}$) try to penetrate the passive layer of the metal surface to form pitting corrosion so that the H-beam steel is in a corroded condition Fe^{2+} (steel will release 2 electrons) .

(3) The ability of Zn zinc sacrificial anode with a level of 99.99% to inhibit the corrosion rate of H-beam steel for 30 days/720 hours at an environmental pH of 6 to 6.5 reaches 50.5%.

REFERENCES

[1] E. Gunawan, "Analisa pengaruh temperatur terhadap sifat mekanis dan struktur mikro pada baja karbon rendah (st41) dengan metode pack carbirizinG," *Tek. Eng. Sains J.*, vol. 1, no. 2, pp. 117–124, Dec. 2017, doi: 10.51804/TESJ.V1I2.133.117-124.

[2] P. Dai, L. Yang, X. Yun, F. Wang, and L. Zhang, "Experimental study of concrete-filled stainless steel tubular stub columns with circular and square cross-sections subjected to combined compression and bending," *Eng. Struct.*, vol. 305, p. 117773, Apr. 2024, doi: 10.1016/J.Engstruct.2024.117773.

[3] K. Setiawan Widana, dan Bambang Priadi, P. Teknologi Bahan Galian Nuklir - BATAN, J. Lebak Bulus Raya No, and P. Jumat, "Karakteristik Unsur Jejak Dalam Diskriminasi Magmatisme Granitoid Pulau Bangka," *EKSPLORIUM*, vol. 36, no. 1, pp. 1–16, May 2015, doi: 10.55981/Eksplorium.2015.2766.

[4] R. '. (Rahmat) Ilham, K. (Komalasari) ', and R. S. (Rozanna) Irianty, "Proteksi Katodik dengan Menggunakan Anoda Korban pada Struktur Baja Karbon dalam Larutan Natrium Klorida," *J. Online Mhs. Fak. Tek. Univ. Riau*, vol. 2, no. 2, pp. 1–6, 2015, Accessed: Mar. 31, 2024. [Online]. Available: https://www.neliti.com/publications/183500/

[5] N. Rukminasari, N. Nadiarti, and K. Awaluddin, "Pengaruh Derajat Keasaman (pH) Air Laut Terhadap Konsentrasi Kalsium dan Laju Pertumbuhan H A L I M E D A SP," *Torani J. Fish. Mar. Sci.*, vol. 24, no. 1, 2014, doi: 10.35911/TORANI.V24I1.119.

[6] B. Tanah di Jalur Krueng Peusangan hingga Krueng Geukueh, A. Utara Reza Putra, S. Huzni, S. Fonna, and N. Diterima, "Pengaruh faktor lingkungan terhadap potensi korosi pada pipa air bawah tanah di jalur krueng peusangan hingga krueng geukueh, aceh utara," *flywheeL J. Tek. Mesin Untirta*, vol. 1, no. 1, pp. 14–19, Apr. 2018, doi: 10.36055/FWL.V1I1.3289.

[7] K. R. (Kenneth R. C. J. W. A. T. K. Trethewey, "Korosi untuk mahasiswa sains dan rekayasa," *(No Title)*, Accessed: Mar. 31, 2024. [Online]. Available: https://cir.nii.ac.jp/crid/1130282269205132928

[8] J. W. Paik, J. K. Cha, Y. W. Song, D. S. Thoma, R. E. Jung, and U. W. Jung, "Effect of Schneiderian membrane integrity on bone formation in sinus augmentation: An experimental study in rabbits," *J. Clin. Periodontol.*, vol. 49, no. 1, pp. 76–83, Jan. 2022, doi: 10.1111/JCPE.13562.

[9] P. A. Games, "Limitations of Analysis of Covariance on Intact Group Quasi-Experimental Designs," *J. Exp. Educ.*, vol. 44, no. 4, pp. 52–54, 1976, doi: 10.1080/00220973.1976.11011551.

[10] M. F. J. Dijkstra, H. Buwalda, A. W. F. De Jong, A. Michorius, J. G. M. Winkelman, and A. A. C. M. Beenackers, "Experimental comparison of three reactor designs for photocatalytic water purification," *Chem. Eng. Sci.*, vol. 56, no. 2, pp. 547–555, Jan. 2001, doi: 10.1016/S0009-2509(00)00259-1.

[11] Philip H. Henning, "Experimental Research Methods," *Handb. Res. Educ. Commun. Technol.*, pp. 1007–1029, Jan. 2013, doi: 10.4324/9781410609519-

51.
[12] J. Fjermestad and S. R. Hiltz, “An Assessment of Group Support Systems Experimental Research: Methodology and Results,” *J. Manag. Inf. Syst.*, vol. 15, no. 3, pp. 7–149, 1998, doi: 10.1080/07421222.1998.11518216.
[13] D. M. Johnson, D. Allason, and P. M. Cronin, “Large scale experimental research of VCEs – A summary from one viewpoint,” *J. Loss Prev. Process Ind.*, vol. 89, p. 105287, Jul. 2024, doi: 10.1016/J.JLP.2024.105287.
[14] L. Texeira, D. Calisaya-Azpilcueta, C. Cruz, Y. L. Botero, and L. A. Cisternas, “Impact of the use of seawater on acid mine drainage from mining wastes,” *J. Clean. Prod.*, vol. 383, p. 135516, Jan. 2023, doi: 10.1016/J.JCLEPRO.2022.135516.
[15] T. Waly, M. D. Kennedy, G. J. Witkamp, G. Amy, and J. C. Schippers, “Predicting and measurement of pH of seawater reverse osmosis concentrates,” *Desalination*, vol. 280, no. 1–3, pp. 27–32, Oct. 2011, doi: 10.1016/J.DESAL.2011.06.057.
[16] A. Ratanpara *et al.*, “Towards green carbon capture and storage using waste concrete based seawater: A microfluidic analysis,” *J. Environ. Manage.*, vol. 345, p. 118760, Nov. 2023, doi: 10.1016/J.JENVMAN.2023.118760.
[17] T. V. Raudina *et al.*, “Colloidal organic carbon and trace elements in peat porewaters across a permafrost gradient in Western Siberia,” *Geoderma*, vol. 390, p. 114971, May 2021, doi: 10.1016/J.GEODERMA.2021.114971.
[18] K. Zidan, L. Mandi, A. Hejjaj, N. Ouazzani, and A. Assabbane, “Soil fertility and agro-physiological responses of maize (Zea mays) irrigated by treated domestic wastewater by hybrid multi-soil-layering technology,” *J. Environ. Manage.*, vol. 351, p. 119802, Feb. 2024, doi: 10.1016/J.JENVMAN.2023.119802.
[19] R. A. M. Williams *et al.*, “Estimating soil health in urban allotments: Integrated two-way soil quality index and free-living amoebae in nitrogen recycling,” *Soil Environ. Heal.*, vol. 1, no. 4, p. 100046, Dec. 2023, doi: 10.1016/J.SEH.2023.100046.
[20] N. Olgun *et al.*, “Lithological controls on lake water biogeochemistry in Maritime Antarctica,” *Sci. Total Environ.*, vol. 912, p. 168562, Feb. 2024, doi: 10.1016/J.SCITOTENV.2023.168562.
[21] P. Castillo *et al.*, “Biogeochemistry of plant essential mineral nutrients across rock, soil, water and fruits in vineyards of Central Chile,” *CATENA*, vol. 196, p. 104905, Jan. 2021, doi: 10.1016/J.CATENA.2020.104905.
[22] M. Vinichuk, R. Bergman, S. Sundell-Bergman, and K. Rosén, “Response of spring wheat and potato to foliar application of Zn, Mn and EDTA fertilizers on 137Cs uptake,” *J. Environ. Radioact.*, vol. 227, p. 106466, Feb. 2021, doi: 10.1016/J.JENVRAD.2020.106466.
[23] A. G. Caporale, M. Palladino, S. De Pascale, L. G. Duri, Y. Rouphael, and P. Adamo, “How to make the Lunar and Martian soils suitable for food production - Assessing the changes after manure addition and implications for plant growth,” *J. Environ. Manage.*, vol. 325, p. 116455, Jan. 2023, doi: 10.1016/J.JENVMAN.2022.116455.
[24] F. Yousefi, T. White, D. R. Lentz, C. R. M. McFarlane, and K. G. Thorne, “Middle Devonian Evandale porphyry Cu-Mo (Au) deposit, southwestern New Brunswick, Canada: Analysis of petrogenesis to potential as a source for

distal intrusion-related epithermal gold mineralization," *Ore Geol. Rev.*, vol. 162, p. 105716, Nov. 2023, doi: 10.1016/J.OREGEOREV.2023.105716.
[25] S. Metz, A. Bertsch, and P. Renaud, "Partial release and detachment of microfabricated metal and polymer structures by anodic metal dissolution," *J. Microelectromechanical Syst.*, vol. 14, no. 2, pp. 383–391, Apr. 2005, doi: 10.1109/JMEMS.2004.839328.
[26] A. Levallois *et al.*, "Aluminium-based galvanic anode impacts the photosynthesis of microphytobenthos and supports the bioaccumulation of metals released," *Aquat. Toxicol.*, vol. 258, p. 106501, May 2023, doi: 10.1016/J.AQUATOX.2023.106501.
[27] Z. Liu, X. Zhang, J. Luo, and Y. Yu, "Application of metal-organic frameworks to the anode interface in metal batteries," *Chinese Chem. Lett.*, p. 109500, Jan. 2024, doi: 10.1016/J.CCLET.2024.109500.